Tuijin Jishu/Journal of Propulsion Technology
ISSN: 1001-4055
Vol. 45 No. 1 (2024)

Optimized Wireless Energy Harvesting: High-Gain Wideband Antenna Integration in Half-wave Rectenna Unit

Pradeep Chandrakant Dhanawade[1], Shivajirao M. Sangale[2]

[1]*Research Scholar, Shivaji University, Kolhapur, 416115, Maharashtra, India.*

[2]*ECE Department, Karamveer Bhaurao Patil College of Engineering, Satara, 415001, Maharashtra, India.*

Abstract: **-** Wireless energy harvesters enable the continuous operation of sensors without the need for frequent battery replacements, ensuring long-term and autonomous functionality in remote or challenging environments. In this work, we have designed and developed a half-wave rectifier for the purpose of wireless energy harvesting and transfer. This rectenna has been specifically designed to operate within the commonly used 2100 MHz wireless band and is powered by a high-gain wideband antenna. The rectifier consists of two surface mount SMS7630 Schottky diodes, a capacitor, and a 1 k**Ω** load resistor. We have achieved the desired operating band by adjusting the dimensions of matched transmission lines. To power the rectenna, we have also designed a high-gain wideband antenna. The antenna's gain has been improved by introducing an air-gap and utilizing a low-loss RT-duroid 5880-based multilayered substrate. Additionally, we have reduced the length of the ground plane to increase the antenna's bandwidth, resulting in an omnidirectional radiation pattern. Both the antenna and rectifier circuits were developed and tested independently. Our proposed rectenna exhibits a measured radio frequency to direct current conversion efficiency of 27.9%.

Keywords*: High-gain antenna, rectenna, low-power half-wave rectifier, wideband antenna, wireless power transfer.*

1. Introduction

In the realm of smart agriculture, the significance of wireless sensor networks lies in their ability to actively monitor key environmental factors like soil moisture, temperature, and crop health in real-time. This facilitates the implementation of precision farming techniques, effectively managing resources and improving crop yields through informed, data-driven decision-making processes [1]. In supporting wireless sensor networks, the essential role of wireless energy harvesters is evident as they transform available ambient energy, such as solar or kinetic energy, into electrical power. This capability ensures the uninterrupted functioning of sensors, eliminating the necessity for frequent battery changes and thereby guaranteeing sustained, autonomous operations even in remote or challenging settings.

A rectenna is the result of merging an antenna with a rectifier circuit, effectively integrating a rectifier within an antenna structure [3]. This unique combination allows the antenna to capture electromagnetic waves and then convey them to the rectifier circuit, where they are transformed into direct current. This technology holds numerous applications in both current and future generations of consumer electronics, including wireless charging for medical implant devices and electronic gadgets. The performance of a rectenna relies on several critical parameters, including antenna gain, directivity, bandwidth, the specific type of rectifier circuit, the active components involved, rectifier losses, and the load characteristics. In particular, crafting a rectenna for wireless energy harvesting poses a significant challenge, primarily due to the stringent requirements of operating at very low power levels. This necessitates avoiding the use of general-purpose diodes due to their higher forward voltage drop.

The literature on wireless power transfer and wireless energy harvesting has seen numerous rectifier designs documented [4], [5-8]. In [2], researchers focused on designing a rectenna tailored for wireless power transfer within the Industrial, Scientific, and Medical (ISM) bands. Their emphasis was on reducing the rectenna's physical footprint and shortening the time required for its realization. Another study in the field of wireless power transfer is presented in reference [4], where a rectenna employing a Schottky diode is developed for the ISM 2.45 GHz band. In this case, the researchers concentrated on achieving enhanced impedance matching between the antenna and the rectifier by incorporating a matching circuit. Reference [5] introduces a high-frequency, multi-band rectenna for wireless energy harvesting. This rectenna incorporates a two-dimensional and flexible antenna, operating within the 2.4 GHz, 5.9 GHz, and 8 to 12 GHz bands. Similarly, reference [6] describes the design of a single-layer, multi-band rectenna optimized for wireless energy harvesting, with operation extending to the millimeter-wave 26 GHz band. For wireless energy harvesting within lower frequency ranges, multi-band rectennas are explored in references [7-8]. These references explore various rectifier circuit configurations, including half-wave [6], full-wave [9-10], and full-wave rectifiers with voltage doubler circuits [11-13], all aimed at enhancing the rectenna's overall efficiency.

2. Objectives

This paper presents the development of wideband high-gain antennas and a half-wave rectifying circuit specifically designed for operation in the 2100 MHz band. Our wideband, high-gain antenna leverages a multilayer substrate and employs partial ground techniques to achieve its performance characteristics. It's important to note that our approach to the half-wave rectifier differs from traditional designs, as we employ two SMS7630 Schottky diodes to enhance the circuit's longevity and efficiency. One diode rectifies the positive half-wave cycle, while the other is responsible for grounding the negative half-cycle. Both the antenna and rectifier circuit undergo thorough simulation and analysis using a full-wave electromagnetic simulator. Furthermore, we have developed physical prototypes to validate our design against the simulation results. The alignment between our simulation and measurement outcomes serves as a strong confirmation of the effectiveness of our proposed approach.

3. Methods

3.1 Half Wave-Rectifier Circuit

In this section, the detailed design and analysis of the half-wave circuit. Our rectifier configuration comprises two SMS7630 Schottky diodes, a 1 µF capacitor, a load resistance, and microstrip stubs. Figure 1 illustrates the configuration of this rectifier.

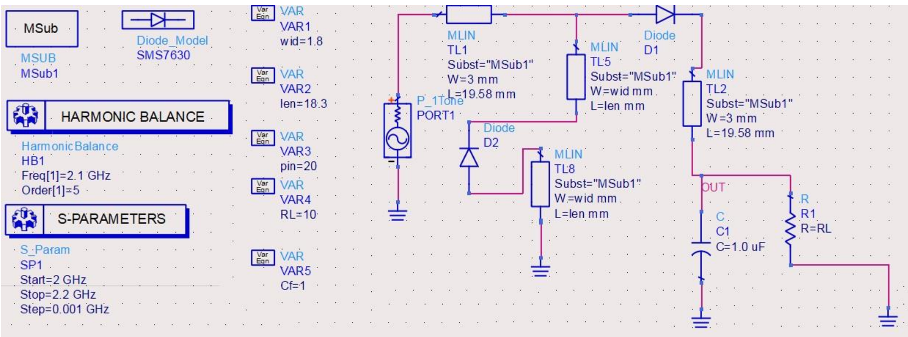

Fig. 1 Half-wave rectifier circuit diagram analysed using ADS.

To power this rectifier, we utilize a single-tone input power source operating at 2100 MHz. Our analysis employs both harmonic balance and scattering parameter techniques to thoroughly investigate the rectifier's conversion efficiency and the impedance matching parameters at the input port. We have meticulously adjusted the dimensions of the microstrip stubs to optimize both the conversion efficiency and the impedance matching characteristics of the rectifier. Figure 2(a) illustrates the relationship between the frequency at the rectifier's input port and its scattering parameter. Notably, the rectifier exhibits resonance precisely at 2100 MHz, encompassing a wideband range from 2080 MHz to 2180 MHz.

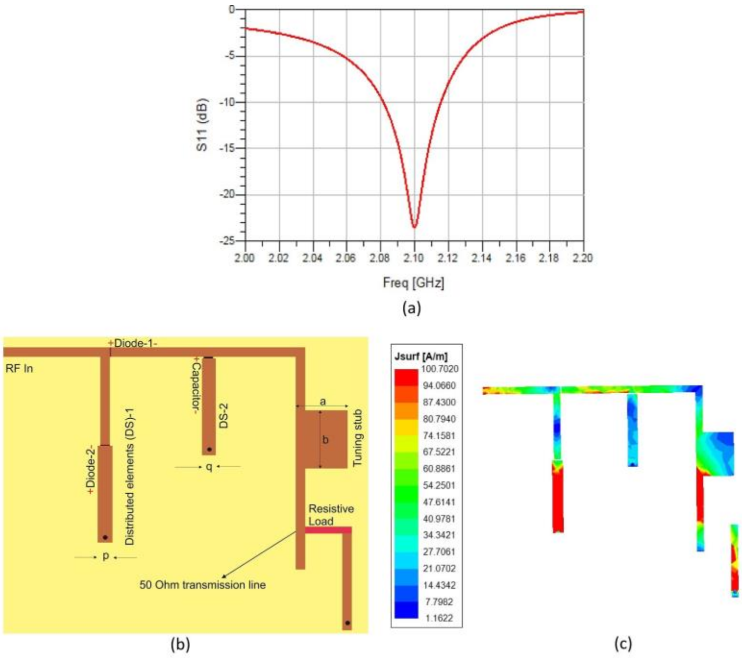

Fig. 2 Half-wave rectifier distributed element layout and performance parameters (a) S11 parameter (b) layout (c) Surface current density.

This results in a substantial 100 MHz bandwidth centered around the pivotal frequency of 2100 MHz. For a more detailed understanding of the rectifier's inner workings, we have devised an equivalent distributed element layout, depicted in Figure 2(b). Within this layout, we employ a model representing the SMS7630 Schottky diode. To ensure precision, we have incorporated specific diode specifications obtained from the manufacturer's technical dataset. Notably, Figure 2(b) distinguishes between two diodes: Diode-1, which serves as the primary rectifying diode, and Diode-2, employed to ground the negative half-cycle. During the positive half-wave cycle, Diode-1 enters a forward-biased state, facilitating the charging of the capacitor. In contrast, Diode-2 remains reverse-biased, effectively behaving as an open switch. The capacitor plays a dual role in filtering the output and delivering a continuous current to the load. It's important to note that, at this stage, the output is characterized by unstable direct current, necessitating further voltage and current regulation to achieve stability and reliability. We have also conducted a validation of the distributed element layout's performance by plotting the surface current, as illustrated in Figure 2(c). This depiction highlights the rectifier configuration's effectiveness, as evidenced by the higher current density observed at the grounding positions within Figure 2(c). We conducted an in-depth analysis of the radio frequency to direct current conversion efficiency of the rectifier, and the results are presented in Figure 3. In Figure 3(a), we examined the rectifier's performance concerning the input

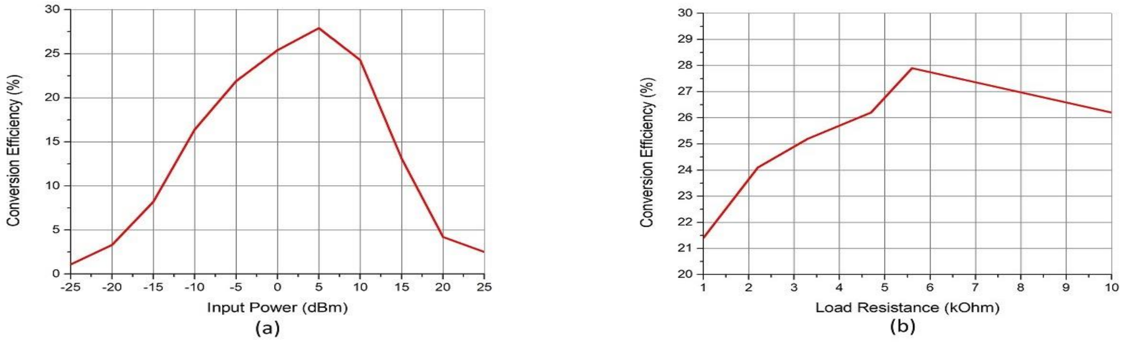

Fig. 3 Conversion efficiency of the half-wave rectifier.

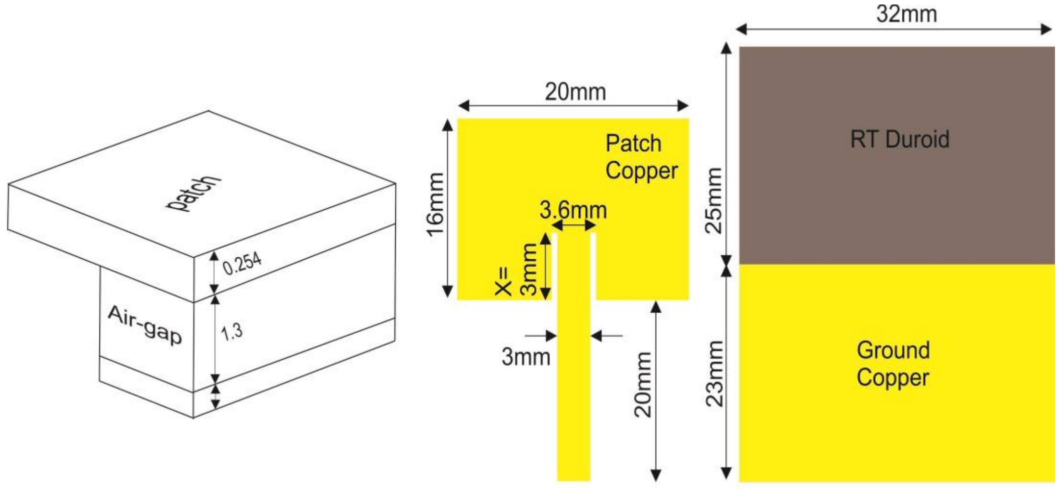

(a) (b)

Fig. 4 Wideband high-gain antenna (a) Substrate (b) Antenna design.

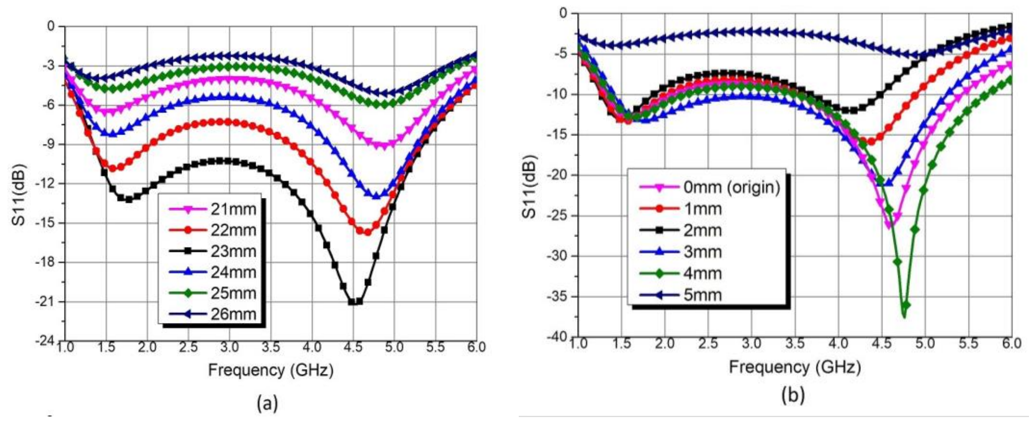

Fig. 5 Reflection coefficient of the wideband antenna (a) Versus ground size (b) Versus feeding position.

power level, while Figure 3(b) illustrates its behavior across a range of resistive loads. Our investigation encompassed a wide input power level spectrum, varying from -25 dBm to +25 dBm, in 5 dBm increments. Throughout this analysis, the load resistor remained fixed at 5.6 kΩ.

Our findings reveal that the rectifier attains its peak conversion efficiency of 27.7% when subjected to an input power level of +5 dBm. However, as the input power level exceeds 5 dBm, the conversion efficiency experiences a decline. To further explore the rectifier's performance characteristics, we also investigated its response to variations in the resistive load, spanning from 1 kΩ to 10 kΩ. It's worth noting that, for the load investigation, we exclusively considered commercially available resistors with values of 1 kΩ, 2.2 kΩ, 3.3 kΩ, 4.7 kΩ, 5.6 kΩ, and 10 kΩ. For these experiments, the input power level remained fixed at 5 dBm. Remarkably, our analysis demonstrated that the rectifier achieves its optimal conversion efficiency when matched with a 5.6 kΩ resistive load, as depicted in Figure 3(b). As the load resistance increases to 10 kΩ, the conversion efficiency experiences a noticeable reduction. These insights offer a comprehensive understanding of the rectifier's performance under various conditions, providing valuable information for its practical application and optimization.

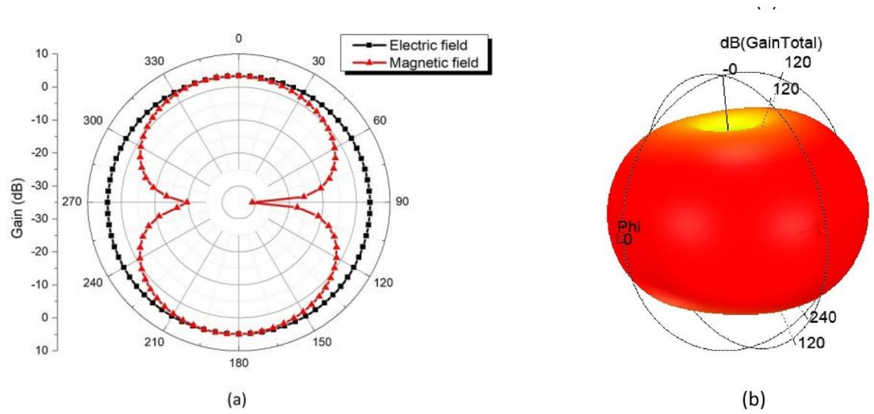

Fig. 6 Radiation patterns of the wideband antenna (a) Two dimensional electric and magnetic field pattern (b) three-dimensional radiation pattern.

3.2 High Gain Wideband antenna

In this section, we present the design of a wideband antenna characterized by high-gain properties. The antenna's structural composition and dimensional specifications are thoughtfully delineated in Figure 4. Our overarching objective is to enhance the antenna's gain by mitigating dielectric losses and effectively reducing the overall dielectric constant of the substrate material. To attain this goal, we have ingeniously fashioned a three-layer substrate configuration. This configuration features two layers of the low-loss RT Duroid substrate, each possessing a thickness of 0.254 mm and a dielectric constant of 2.2. Notably, this substrate exhibits an exceptionally low loss tangent of merely 0.0002, thereby minimizing signal attenuation. Of particular significance is the introduction of a 1.3 mm air-gap positioned between the two layers of the RT Duroid substrate. This deliberate incorporation of an air-gap serves a dual purpose: firstly, it substantially diminishes the overall dielectric constant of the resulting three-layer substrate, which in turn has the effect of reducing the effective dielectric losses. Secondly, this ingenious arrangement contributes significantly to the augmentation of the antenna's gain characteristics. The configuration of these three substrate layers is meticulously depicted in Figure 4(a), affording a clear visual representation of our design. Notably, at the base of the substrate, we have incorporated a partial substrate section, which plays a pivotal role in constraining the ground plane to specific dimensions. This strategic limitation of the ground plane is instrumental in achieving the desired wider bandwidth for the antenna, a critical performance criterion for its intended applications.

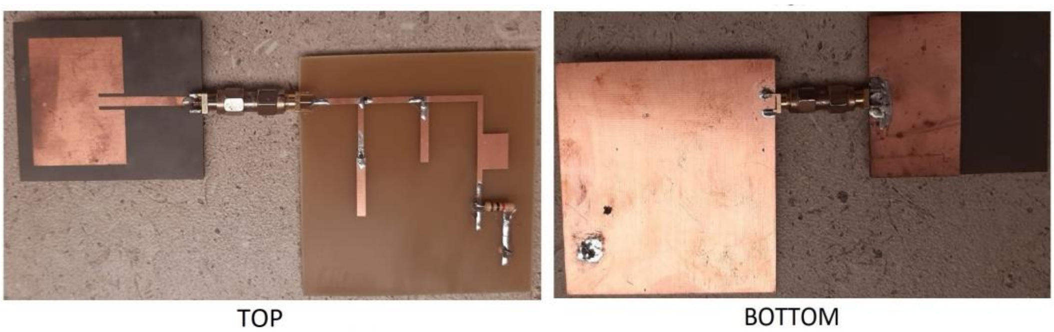

Fig. 7 Fabricated proposed rectenna model.

The ground plane length is fixed to 23 mm after performing the investigation. The investigation results are shown in Figures 5(a) and 5(b). The investigation concentrates on the impedance matching affected by the ground length and the co-planar waveguide feed location.

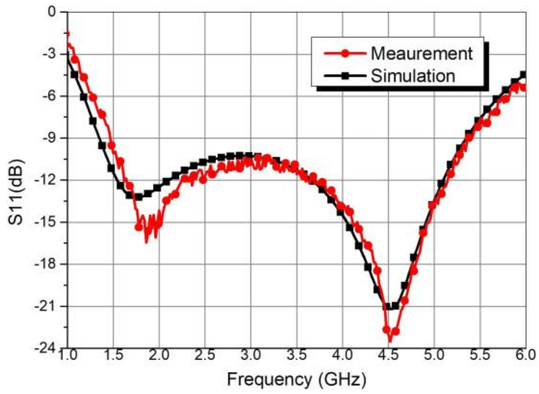

Fig. 8 Simulation and measurement S11 of the wideband antenna.

The ground length of the antenna is varied from 21 mm to 26 mm with step size of 1 and scattering parameters are plotted in Figure 5(a). It is found that, for ground length 23 mm the antenna has wider bandwidth from 1400 MHz to 5200 MHz. Thus, the ground length is set to 23 mm. For larger or smaller ground length the antenna has narrowband in upper frequency range.

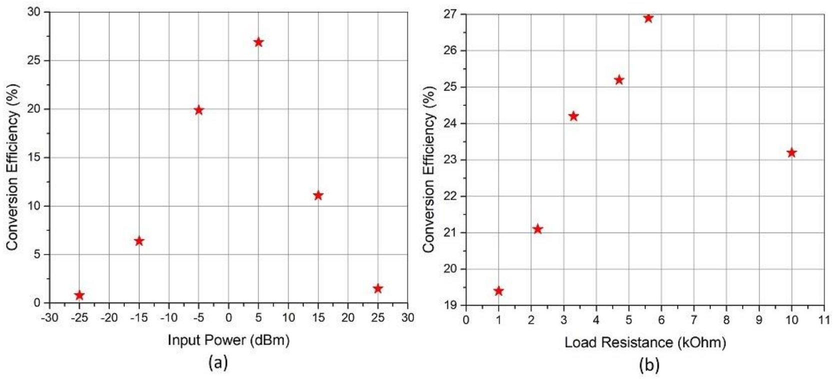

Fig. 9 Measurement results of rectenna (a) versus input power (b) versus load.

4. Results

The prototype of the antenna and the half-wave rectifier is fabricated and shown in Figure 7. The upper and lower layer of the antenna is fabricated on RT Duroid o.254 mm thick substrate. The upper layer is a patch of the antenna and the lower layer is partial ground. After etching the lower layer as per ground plane length, it is cut to realize the proposed multilayer structure, as shown in Figure 7. The fabricated antenna is tested and the scattering parameter result is shown in Figure 8. The measured scattering parameter is perfectly matched to the simulated scattering parameter. The antenna has a wideband matching with a lower -10 dB lower cut-off frequency at 1500 MHz and upper cut-off frequency at 5250 MHz. In this entire band, the antenna has S11 below -10 dB. The gain of the antenna is measured at a single 2100 MHz frequency and found at 7.4 dBi. The fabricated half-wave rectifier is connected to this antenna using a male-to-male sub-miniature-type-A connector, as shown in Figure 7. To test the rectifier efficiency, 20 dBm of power is radiated from the radio frequency source using a horn antenna. The rectifier is found working well and a voltage drop of 0.62 V is observed in the load resistor. However, when this rectifier will be fed through a highly directive narrowband antenna, much better results are expected.

5. Discussion

A half-wave low-power rectifier using Schottky diodes is presented and its performance analysis is investigated for wireless energy harvesting/transfer applications. The input power level and the operating load are found two important factors affecting the rectifier's performance. Each new rectifier needs optimal power and load to give its best performance. Rectifier exhibits poor performance for lower as well as higher power levels and loads. A moderate power level and load deflect the best conversion efficiency. To feed this rectifier, a wideband monopole antenna with a shortened ground is also designed and analysed. The shortening of the ground plane results in monopole radiation but wider bandwidth. The proposed rectenna performs satisfactorily for wireless energy harvesting or transfer application.

Declaration statements

No funding has been received for this work. Authors has no conflicts of interest/competing interests.

Data sharing not applicable to this article as no datasets were generated or analysed during the current study.

No code is available for this work.

Refrences

[1] G. Sahitya, N. Balaji and C. D. Naidu," Wireless sensor network for smart agriculture," 2016 2nd International Conference on Applied and Theoretical Computing and Communication Technology (iCATccT), Bangalore, India, 2016, pp. 488-493, doi: 10.1109/ICATCCT.2016.7912049.

[2] Kumar, J., Kumar, R., Basu, B., Talukdar, F A., Kumar, A. "Design Challenges of Rectenna for Energy Harvesting from Microwave Pollution," Asian Journal of Water, Environment and Pollution, Vol. 16, 2019, doi:10.3233/AJW190015.

[3] Marriwala, N. Energy Harvesting System Design and Optimization Using High Bandwidth Rectenna for Wireless Sensor Networks. Wireless Pers Commun 122, 669–684 (2022). https://doi.org/10.1007/s11277-021-08918x

[4] Keerthana, S, Uthranarayan, V, Rajalakshmi, Ramya, A. "Wireless Power Transfer Using Rectenna," Journal of Physics: Conference Series, Vol. 1362, 2019, doi:10.1088/1742-6596/1362/1/012037.

[5] Zhang, X. et al. "Two-dimensional MoS2-enabled flexible rectenna for Wi-Fi-band wireless energy harvesting," Nature, Vol. 566, 2019, Smart agriculture energy harvesting. doi:10.1038/s41586-019-0892-1.

[6] Heba A, S., Abdelhalim A Z. "Compact and High-Efficiency Rectenna for Wireless Power-Harvesting Applications," International Journal of Antennas and Propagation, Vol. 2021, 2021, doi:10.1155/2021/1109850.

[7] Achilles D. B. et al. "Triple-Band Single-Layer Rectenna for Outdoor RF Energy Harvesting Applications," Sensors, Vol. 21, 2021, doi:10.3390/s21103460.

[8] Nguyen, D A., Bui, G T., Nam, H., Seo, C. "Design of DualBand Inverse Class-F Rectifier for Wireless Power Transfer and Energy Harvesting," IEEE Microwave and Wireless Technology Letters, doi:10.1109/LMWC.2022.3217459.

[9] F. Erkmen, T. S. Almoneef and O. M. Ramahi "Electromagnetic Energy Harvesting Using Full-Wave Rectification," IEEE Transactions on Microwave Theory and Techniques, vol. 65, 2017, doi:10.1109/TMTT.2017.2673821.

[10] M. Mattsson, C. I. Kolitsidas and B. L. G. Jonsson "Dual-Band DualPolarized Full-Wave Rectenna Based on Differential Field Sampling," IEEE Transactions on Microwave Theory and Techniques, vol. 17, 2018, doi:10.1109/LAWP.2018.2825783.

[11] T. Mitani, S. Kawashima and T. Nishimura "Analysis of Voltage Doubler Behavior of 2.45-GHz Voltage Doubler-Type Rectenna," IEEE Antennas and Wireless Propagation Letters, vol. 65, 2017, doi:10.1109/TMTT.2017.2668413.

[12] M. -J. Nie, X. -X. Yang, G. -N. Tan and B. Han "A Compact 2.45-GHz Broadband Rectenna Using Grounded Coplanar Waveguide," IEEE Antennas and Wireless Propagation Letters, vol. 14, 2015, doi:10.1109/LAWP.2015.2388789.

[13] V. D. Pham, H. Takhedmit and L. Cirio "Waveform Optimization Using RF Pulse Signal on Voltage-Doubler Broadband Rectenna," IEEE Journal of Radio Frequency Identification, vol. 5, 2021, doi:10.1109/JRFID.2020.3039878.